J|A|C|S

A R T I C L E S

One- and Two-Photon Induced Polymerization of Methylmethacrylate Using Colloidal CdS Semiconductor Quantum Dots

Nicholas C. Strandwitz,[†] Anzar Khan,[‡] Shannon W. Boettcher,[§]
Alexander A. Mikhailovsky,[§] Craig J. Hawker,[†,‡,§] Thuc-Quyen Nguyen,[§] and
Galen D. Stucky*,[†,‡,§]

Materials Department, Department of Chemistry and Biochemistry, and Materials Research Laboratory, University of California Santa Barbara, Santa Barbara, California 93106

Received December 20, 2007; E-mail: stucky@chem.ucsb.edu

Abstract: The development of one- and two-photon induced polymerization using CdS semiconductor quantum dots (QDs) and amine co-initiators to promote radical generation and subsequent polymerization is presented. Two-photon absorption (TPA) cross-section measurements, linear absorption, and transmission electron microscopy are used to characterize the QDs. The effectiveness of the co-initiators in increasing the efficiency of photopolymerization (polymer chains formed per excitation) is examined. Triethylamine was observed to be most effective, yielding quantum efficiencies of initiation of >5%. The interactions between the co-initiators and QDs are investigated with steady-state photoluminescence and infrared spectroscopies. Possible initiation mechanisms are discussed and supported by electrochemical data. Making use of the surface chemistry developed here and the large QD TPA cross-sections, two-photon induced polymerization is demonstrated. The large TPA cross-sections coupled with modest quantum efficiencies for initiation reveal the unique potential of molecularly passivated QDs as efficient two-photon photosensitizers for polymerization.

1. Introduction

Two-photon absorption (TPA) is a nonlinear optical process whereby the simultaneous absorption of two photons causes a single excitation of a semiconductor or molecule.[1] The TPA rate is proportional to the square of the incident light intensity. This fact enables the three-dimensional (3D) addressability of excitations within a given material under focused laser exposure with a spatial resolution approaching the diffraction limit (typically ~800 nm). Because excitations can be controlled in 3D, any excitation products (e.g., fluorescence or chemical transformations) can also be controlled in 3D. This spatial addressability enables remarkable applications including 3D data storage,[2] photoimaging,[3] photodynamic therapy,[4] and 3D nanolithography.[5–7] Several of these applications (nanolithography and, in some cases, data storage) rely on two-photon excitation to induce polymerization of nearby monomers. This process is known as two-photon induced polymerization (TPIP) and is the focus of this work.

The efficiency of a TPIP system depends largely on two figures of merit: the absorber TPA cross-section (δ) and the fraction of excitations resulting in polymer initiation (Φ_o).[8] Ideally, absorbers are efficiently excited by the simultaneous absorption of two photons (large δ) and these excitations efficiently initiate polymerization reactions (large Φ_o). Radical-based polymerization mechanisms are especially suited for TPIP because they provide an amplification of the photoinduced process by adding many monomers to a growing polymer chain (or network) for each photosensitized initiation event.

TPIP has been previously reported using organic photoinitiators[5] (which decompose to form radicals) and photosensitizers[7] (which generate radicals by excited-state charge transfer). Using commercial photoinitiators with small TPA cross-sections (typically, δ < 1 GM), Kawata et al. have shown that TPIP can be used to write 3D polymeric structures with subdiffraction resolution of 120 nm under tight-laser focusing conditions.[5] Perry and Marder et al. have shown that TPIP using large-TPA cross-section (δ = 1250 GM) D-π-D photosensitizers (where D is a donor and π is a π-conjugated bridge) allows for more efficient and lower-threshold TPIP.[7] However, the fraction of excited states that result in polymer formation for these molecules is fairly low (Φ_o = 0.03).[9] These reports suggest that increasing initiation efficiencies and absorber TPA cross-sections will increase the overall efficiency of a TPIP system.

[†] Materials Department.
[‡] Materials Research Laboratory.
[§] Department of Chemistry and Biochemistry.
(1) Goeppert-Mayer, M. *Ann. Phys.* **1931**, *9*, 273.
(2) Parthenopoulos, D. A.; Rentzepis, P. M. *Science* **1989**, *245*, 843.
(3) Larson, D. R.; Zipfel, W. R.; Williams, R. M.; Clark, S. W.; Bruchez, M. P.; Wise, F. W.; Webb, W. W. *Science* **2003**, *300*, 1434.
(4) Fisher, W. G.; Partridge, W. P.; Dees, C.; Wachter, E. A. *Photochem. Photobiol.* **1997**, *66*, 141.
(5) Kawata, S.; Sun, H. B.; Tanaka, T.; Takada, K. *Nature* **2001**, *412*, 697.
(6) Belfield, K. D.; Schafer, K. J.; Liu, Y. U.; Liu, J.; Ren, X. B.; Van Stryland, E. W. *J. Phys. Org. Chem.* **2000**, *13*, 837.
(7) Cumpston, B. H.; et al. *Nature* **1999**, *398*, 51.

(8) LaFratta, C. N.; Fourkas, J. T.; Baldacchini, T.; Farrer, R. A. *Angew. Chem., Int. Ed.* **2007**, *46*, 6238.
(9) Marder, S. R.; Brédas, J.-L.; Perry, J. W. *Mater. Res. Bull.* **2007**, *32*, 561.

Semiconductor quantum dots (QDs), with δ values approaching 5×10^4 GM,[3] are excellent candidates for TPIP photosensitizers. These increased TPA cross-sections allow for an increase in the two-photon excitation rate by a factor of 50−5000 over conventional TPA materials under given excitation conditions. However, the TPIP process relies not only on excitation but also on the transformation of excitations into polymerization reactions. That is, it is critical to efficiently channel QD excitations into polymer initiation (i.e., to increase Φ_o) for QDs to be realized as efficient TPIP photosensitizers. The use of QDs as photosensitizers for TPIP has not previously been reported, so information regarding initiation efficiencies for QD-based TPIP systems is unavailable.

Reports of semiconductor and semiconductor particulate photoinitiated polymerization, however, provide insight into the photochemistry available for initiation because excitations in QDs resulting from one- and two-photon absorption are equivalent (both result in the generation of an electron−hole pair).[10–21] Previous research involving the use of photoexcited semiconductors as photosensitizers for polymerization under linear absorption conditions began with the photopolymerization of methyl methacrylate (MMA) on illuminated ZnO surfaces.[10] A radical−anion initiation mechanism mediated by excited $\cdot O_2^-$ at the ZnO surface along with a free-radical chain propagation mechanism was proposed. Hoffman and Hoffmann utilized quantum-sized CdS, ZnO, and TiO$_2$ stabilized by an ionic double layer for polymerization of MMA[15] and various vinylic monomers[16] in a solvent−monomer system. A strong dependence on solvent was observed along with a strong inhibition due to dissolved oxygen. It was proposed that the initiation mechanism involved the generation of radicals by some combination of monomer reduction and alcohol (solvent) oxidation. These reports were the first to use high-surface-area and low-scattering semiconductor particulate solutions. However, the semiconductor particles were electrostatically stabilized, which leads to an ill-defined semiconductor surface and precludes ligand exchange, thereby preventing solubilization in a variety of solvent−monomer systems. Very recently, photopolymerization of an ionic liquid monomer has been demonstrated by photoinduced electron transfer from CdTe nanocrystals to a diphenyliodinium salt.[21] Chemical surface modification and the use of surface-bound co-initiators to promote radical generation (i.e., increase Φ_o) have not been reported.

In the present work, we demonstrate the use of ligand-passivated CdS QDs as photosensitizers for polymerization of MMA. First, we characterize the optical properties of the oleic acid-capped QDs to verify monodispersity and large, wavelength-dependent δ values. Next, we examine the ability of co-initiators to increase photopolymerization initiation efficiency (Φ_o). The co-initiator-enhanced polymerization system is then used to demonstrate QD-based TPIP. The interactions between the QDs, co-initiators, and monomer are probed by steady-state fluorescence quenching, FTIR, and electrochemistry, which provide a basis for discussion of possible photoinitiation mechanisms.

2. Experimental Section

Chemicals. Cadmium oxide (99.99+%), sulfur (99.98%), oleic acid (tech. 90%), 1-octadecene (tech. 90%), triethylamine (99.5%), diethylamine (99.5+%), *n*-butylamine (99%), 4-dimethylaminopyridine (99%), *N,N*-diethylethylenediamine (99%), and methylmethacrylate (99% with monomethyl ether hydroquinone) were obtained from Aldrich. Acetone, toluene, tetrahydrofuran (THF), methanol, hydrochloric acid (37% in H$_2$O), and fluorescein were obtained from Fluka. Deuterated chloroform and THF were obtained from Cambridge Isotope Laboratories. 2,6-Diisopropyl-*N,N*-dimethylaniline was obtained from Spectragroup Limited Inc. All reagents were used as received except inhibitor was removed from MMA by passing through an alumina column.

CdS QD Synthesis. CdS QDs were synthesized by the methods of Peng et al.[22] Briefly, 0.051 g of CdO, 1.8 mL of oleic acid, and 18.1 mL of octadecene (ODE) were loaded into a 3-neck flask and heated to 295 °C under argon with rapid stirring. Next, 10 mL of ODE containing 6.4 mg of dissolved sulfur were rapidly injected to the stirring Cd-oleate precursor. After 2−5 min of growth at 250 °C, the solution was cooled to room temperature and precipitated with acetone. The QDs were then redissolved in toluene and precipitated with methanol. The toluene/methanol washing was repeated two more times. It was found that the extraction procedure used previously by Peng et al.[22] is unsuitable as it greatly decreases fluorescence quantum yield due to the exposure of the QDs to chloroform.

Linear Photopolymerization. Photopolymerization experiments were conducted as follows: A given mass of QDs (dissolved in toluene) was added to a vial or glass cuvette, and the toluene was subsequently removed under vacuum. It was found that vacuum treatment did not adversely affect subsequent (oleic acid-capped) QD solubility. The QDs were redispersed in MMA ([QDs] = 6.4 $\times$ 10^{-6} mol QD/L), and the solution was purged with argon for several minutes. The previously argon-purged co-initiator (277 mM in monomer) was added to the solution and purged for an additional minute with argon and then sealed. A light-emitting diode light source (λ = 400 nm) was used to irradiate the samples with an incident power of 2.15 mW determined by radiometry (Newport 2930C Power Meter with a calibrated Si detector). A reflection-attenuated power of 2.08 mW was used to calculate quantum yields. Reactions were carried out at room temperature with stirring. Aliquots were removed at given time intervals under argon and were then dissolved in deuterated solvent for NMR analysis. Alternatively, final reaction mixtures were weighed, precipitated with methanol, and washed with a methanol/HCl solution (20:1 v/v) to dissolve and remove the CdS QDs. The polymer was then redissolved in THF, washed twice with methanol, and dried under vacuum. The isolated polymer was then weighed and compared with that of the crude reaction mixture to determine the mass yield.

Two-Photon Polymerization. Two-photon induced polymerization was conducted using identical solutions to those in the linear polymerization experiments but the QD concentration was increased to 8.9 $\times$ 10^{-6} mol QD/L and the co-initiator concentration was increased to 384 mM, so that the molar ratio of co-initiator to QD was the same as that used for linear photopolymerization. A Ti:sapphire femtosecond regenerative amplifier (Spectra Physics

(10) Kuriacose, J.; Markham, M. C. *J. Phys. Chem.* **1961**, *65*, 2232.

(11) Kraeutler, B.; Reiche, H.; Bard, A. J.; Hocker, R. G. *J. Polym. Sci., Part C: Polym. Lett.* **1979**, *17*, 535.

(12) Funt, B. L.; Tan, S. R. *J. Polym. Sci., A: Polym. Chem.* **1984**, *22*, 605.

(13) Kamat, P. V.; Basheer, R.; Fox, M. A. *Macromolecules* **1985**, *18*, 1366.

(14) Kamat, P. V.; Todesco, R. V. *J. Polym. Sci., Part A: Polym. Chem.* **1987**, *25*, 1035.

(15) Hoffman, A. J.; Yee, H.; Mills, G.; Hoffmann, M. R. *J. Phys. Chem.* **1992**, *96*, 5540.

(16) Hoffman, A. J.; Mills, G.; Yee, H.; Hoffmann, M. R. *J. Phys. Chem.* **1992**, *96*, 5546.

(17) Huang, Z. Y.; Barber, T.; Mills, G.; Morris, M. B. *J. Phys. Chem.* **1994**, *98*, 12746.

(18) Popovic, I. G.; Katsikas, L.; Muller, U.; Velickovic, J. S.; Weller, H. *Macromol. Chem. Phys.* **1994**, *195*, 889.

(19) Popovic, I. G.; Katsikas, L.; Weller, H. *Polym. Bull.* **1994**, *32*, 597.

(20) Stroyuk, A. L.; Granchak, V. M.; Korzhak, A. V.; Kuchmii, S. Y. *J. Photochem. Photobiol., A* **2004**, *162*, 339.

(21) Nakashima, T.; Sakashita, M.; Nonoguchi, Y.; Kawai, T. *Macromolecules* **2007**, *40*, 6540.

(22) Yu, W. W.; Peng, X. G. *Angew. Chem., Int. Ed.* **2002**, *41*, 2368.
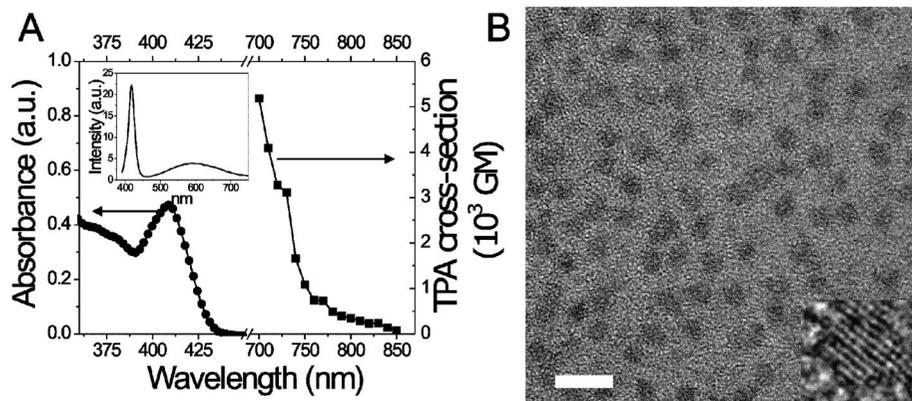
Figure 1. One- and two-photon QD absorption and emission spectra, TEM micrograph. (A) Linear absorption (●) shows a blue-shifted first-exciton absorbance peak relative to bulk CdS (~512 nm) of the QDs in toluene. The TPA cross-sections (■) increase strongly at photon energies above which TPA is allowed, i.e. $h\nu > E_g/2$. (Inset) Both band-edge and trap emission are observed near 410 and 600 nm, respectively, for as-purified QDs in toluene. (B) TEM micrograph of QDs confirming monodispersity and nonagglomerated nature. Scalebar = 10 nm. (Inset) Magnified image of a single CdS QD showing single-crystalline structure.

Spitfire) was used as the light source. The laser was operated at 800 nm, and the light intensity was controlled by neutral density filters. Other parameters were as follows: pulse duration = 1.4 × 10^{-13} s, Gaussian beam radius = 0.13 cm, frequency = 10^3 Hz. The sample was purged with argon and placed in a hermetically sealed, rectangular quartz cell with optical path-length of 1 cm. The sample was illuminated by a collimated laser beam and stirred during the irradiation.

Characterization Methods. QD TPA cross-sections were determined by first measuring fluorescence quantum efficiency of the QDs relative to a fluorescein standard (pH 12, peak linear absorbance = 0.2−0.5) under linear excitation. Quantum yield values measured on our system in this absorbance range vary negligibly from values obtained with more dilute solutions. The integrated two-photon fluorescence intensity under mode-locked, femtosecond Ti:sapphire laser exposure was then compared between the QDs and fluorescein (δ = ~36 GM at 800 nm) to determine the QD TPA cross-sections as reported previously.[23,24]

Fourier transform infrared (FTIR) characterization of QD films treated with co-initiators or monomer was conducted by first drop-casting QDs from toluene onto double-sided-polished n-type Si wafer (1−10 Ω·cm) and drying under vacuum. The dry QD films were then immersed in argon-purged ethanolic solutions of the co-initiators (~1 M) for 24 h, rinsed thoroughly with ethanol, dried under an argon stream, and measured immediately.

Quantum efficiency of chain initiation for linear polymerization was determined by first determining the number of polymer chains in the sample,[25]

$$\Sigma N_x = \frac{w}{\bar{M}_n} \tag{1}$$

where w is the mass of isolated polymer and $\bar{M}_n$ is the number-average molecular weight determined by GPC analysis. The number of polymer chains is then divided by the number of photons absorbed by the sample to determine the quantum efficiency of chain initiation,

$$\Phi_o = \frac{\Sigma N_x}{N_{h\nu}} \tag{2}$$

For TPIP, $N_{h\nu}$ is substituted with the calculated number of excitations under two-photon excitation, which is the product of

illumination time (t) and the estimated excitation rate ($t \cdot \Delta N_{TPA}$), as calculated below. Quantum yield calculations neglect any chain transfer to monomer, which would result in more than one polymer chain per photon and neglect termination by coupling, which would result in one polymer chain per two excitations. Under both linear and two-photon excitation, the reported quantum yield values are artificially lower because of polymer lost during precipitation. This discrepancy due to incomplete precipitation was observed: conversion values by NMR integration were typically ~10% larger than conversion values determined gravimetrically. All quantum yield values reported are based on gravimetric yields and not NMR integrated yields.

A Cary 14 UV−vis-NIR spectrometer was used to acquire absorption spectra of monomer, co-initiators, and QDs. UV−vis absorption was used to determine QD concentrations and particle sizes based on the first exciton absorbance value and the first exciton absorbance peak spectral location.[26] An FEI Tecnai G2 Sphera TEM operating at 200 kV was used to characterize the QD size and crystallinity. QD emission spectra were recorded using PTI Quantum Master fluorimeter relative to a fluorescein standard. PMMA molecular weights and polydispersity were determined using a Waters Alliance High Performance Liquid Chromatography (HPLC) Gel Permeation Chromatography (GPC) System calibrated to PMMA standards using THF as solvent. Polymer yields were determined by NMR or by weighing the isolated polymer. Yields from NMR analysis were computed by comparing integrated PMMA and MMA peaks. All NMR spectra were recorded in deuterated chloroform or deuterated THF using a Bruker Avance 500 spectrometer operating at 500 MHz. FTIR spectra were recorded using a Nicolet Magna-IR 850 Series II Spectrometer.

3. Results and Discussion

QD Characterization. The CdS QDs display well-defined optical features corresponding to a blue-shifted bandgap (E_g = 3.0 eV) with respect to bulk CdS due to quantum confinement (Figure 1A). The sharp fluorescence emission peak (Figure 1A, inset) and multiple absorption peaks observed, along with the transmission electron micrographs (Figure 1B), are evidence of a narrow size distribution (diameter ≈ 3.7 nm). Large CdS QD TPA cross-sections (δ = 5.0 × 10^3 (±10%) GM here and up to δ = 3.5 × 10^4 (±10%) GM at shorter wavelengths, see Supporting Information) are observed at photon energies slightly above $E_g/2$. These large δ values provide motivation for the

(23) Xu, C.; Webb, W. W. *J. Opt. Soc. Am. B* **1996**, *13*, 481.
(24) Wecksler, S. R.; Mikhailovsky, A.; Korystov, D.; Ford, P. C. *J. Am. Chem. Soc.* **2006**, *128*, 3831.
(25) Odian, G. *Principles of Polymerization*, 3rd ed.; John Wiley & Sons, Inc.: New York, 1991.

(26) Yu, W. W.; Qu, L. H.; Guo, W. Z.; Peng, X. G. *Chem. Mater.* **2004**, *16*, 560.
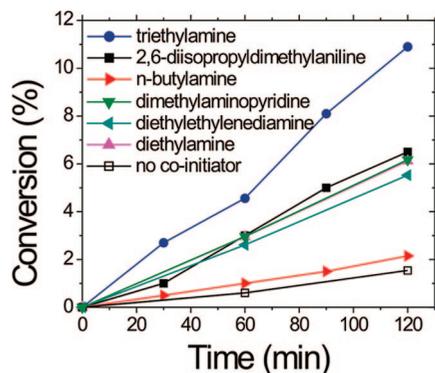
Figure 2. Conversion of MMA to PMMA versus time. Polymerization under linear (λ_{exc} = 400 nm) excitation with various nitrogen-containing co-initiators. Under the conversion regimes explored, conversion was linear with time.

Table 1. Efficiencies and Properties of One- and Two-Photon QD Photopolymerized PMMA

	A. Linear Excitation[a]				
coinitiator	Φ_o (%)	M_w (kDa)	M_n (kDa)	PDI	Conv. (%)
none	0.40 ± 0.02	292	160	1.82	1.5 ± 0.1
n-butylamine	0.79 ± 0.04	244	109	2.23	2.1 ± 0.1
diethylamine	1.8 ± 0.1	222	100	2.22	6.4 ± 0.1
2,6-diisopropyl dimethylaniline	2.2 ± 0.1	228	112	2.04	6.5 ± 0.1
triethylamine	5.2 ± 0.2	144	67.6	2.13	10.9 ± 0.2
diethylethylene diamine	1.0 ± 0.1	178	83.5	2.13	5.5 ± 0.1
4-dimethylamino pyridine	2.3 ± 0.1	188	87.4	2.15	6.2 ± 0.1

		B. Two-Photon Excitation[b]				
power (mW)	Φ_o (%)	M_w (kDa)	M_n (kDa)	PDI	Conv. (%)	illumination time (min)
230	1.7 ± 0.2	175	71.0	2.46	0.38 ± 0.02	180
300	2.0 ± 0.2	195	87.5	2.24	0.95 ± 0.04	180
480	2.2 ± 0.2	215	97.5	2.20	2.1 ± 0.1	120
700	2.1 ± 0.2	216	99.6	2.17	2.0 ± 0.1	60

[a] Initiation efficiency (Φ_o), weight average molecular weight (M_w), number average molecular weight (M_n), polydispersity (PDI), and percent conversion after 2 h illumination with various co-initiators. [b] Initiation efficiency for two-photon induced polymerization at different laser intensities with triethylamine as co-initiator, properties of the resulting polymers, percent conversion, and illumination time (λ = 800 nm, δ = 343 GM).

Figure 3. Chemical structures and names of the co-initiators employed in this work.

use of QDs as two-photon photosensitizers. The CdS QD fluorescence spectrum exhibits features due to band-edge recombination and recombination via trap states. Band-edge recombination results in a narrow emission spectrum and occurs when all the band-edge energy is consumed for photon emission. Recombination via trap states results in a broad emission spectrum and occurs when an electron (or hole) initially decays nonradiatively to a trap state within the bandgap and then relaxes radiatively with a low quantum yield. The trap states in this work are all considered to be "deep" trap states, because the trap state is separated from the valence and conduction bands by energies much greater than k_BT. The broad trap emission peak is observed from 500−700 nm, and a narrow band-edge emission peak is observed at 420 nm.

Linear Photopolymerization. Because one- and two-photon absorption result in the same QD excited state, we chose to initially investigate QD-sensitized photopolymerization of MMA under one-photon (linear) absorption conditions. Here, we study bulk monomers as they closely imitate the photopolymerization of films of multifunctional (meth-) acrylate oligomers and monomers and remove complications introduced by solvent.[16] Further, conducting the photopolymerizations in neat mono-functional monomer allows for facile polymer characterization and calculation of yields and efficiencies. Control polymerization experiments were conducted without QDs, with pure (inhibitor free) MMA monomer, and with solutions in the dark, none of which yielded any measurable amount of polymer. The CdS QDs and co-initiators are both very soluble in MMA, forming homogeneous nonscattering solutions.

Photopolymerization was observed in illuminated solutions containing MMA monomer and unmodified, oleic acid-capped QDs (Figure 2, □, and Table 1A). However, without surface co-initiators present, polymerization is inefficient (Φ_o = 0.4%), indicating that QD excitations are not efficiently translated into propagating polymerization reactions. The resulting polymers have a relatively large molecular weight, which is attributed to a low bimolecular termination rate due to a lower concentration of propagating radicals.[25]
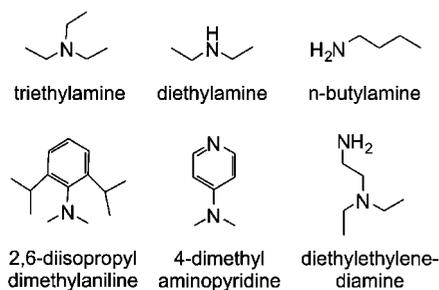
Due to the inefficient photopolymerization observed using unmodified QDs, co-initiator modification of the QD surface was investigated. We hypothesize that, because the QDs have a large surface-area-to-volume ratio and photoexcited carriers are inherently at these surfaces, the state of these semiconductor surfaces will greatly influence the probability of photoinitiation reactions. Various amines were selected as co-initiators due to

their chemical affinity for the QD surface and their routine use in radical photopolymerizations. A structure−function relationship is developed by examining parameters (Figure 3) including the number of substituents on the amine [*n*-butylamine, diethylamine, and triethylamine], the chemical structure and the size of the substituents [triethylamine, diethylethylenediamine, 2,6-diisopropyldimethylaniline, and 4-dimethylaminopyridine], and additional functionality of the substituent [diethylethylenediamine and 4-dimethylaminopyridine].

When co-initiators are employed in photopolymerization experiments, the initiation efficiencies increase dramatically. The initiation efficiency is doubled (Φ_o = 0.8%) when *n*-butylamine is employed as a co-initiator relative to photopolymerization without co-initiators. Polymerization using diethylamine as co-initiator increases Φ_o to 1.7%. Further increases in initiation efficiency are typically observed when tertiary amines are employed relative to primary and secondary amines. Triethylamine yields the highest initiation efficiency in these systems (Φ_o > 5%) with other *tert*-amine co-initiators giving slightly lower values. The molecular weights of the resulting polymers generally decrease with increasing initiation efficiency and is justified as above: higher initiation efficiencies result in an

increased density of propagating radicals, increasing bimolecular termination rates, and thus decreasing polymer molecular weight.

Two-Photon Induced Polymerization. On the basis of the linear photopolymerization results above and the assumption that both TPA and linear absorption result in the generation of the same QD excited state, we investigated the ability of QDs to act as two-photon sensitizers for polymerization. Calculation of initiation quantum efficiency values requires knowledge of the two-photon excitation rate of the sample. Under two-photon excitation, the rate of the excited states generation per unit area of the laser beam cross-section is

$$\Delta n_{TPA} = \frac{CL\delta I_o^2}{2(1 + CL\delta I_o)} \tag{3}$$

where C is the concentration of nonlinear absorbers (particles/cm^3), L is the path length of illumination (cm), δ is the TPA cross-section (10^{-50} cm^4 s photon^{-1} molecule^{-1} = 1 GM), and I_o is the intensity of the incident light (photon cm^{-2} s^{-1}). If the reduction of the excitation light intensity due to multiphoton absorption processes is negligible, then $CL\delta I_o \ll 1$ and eq 3 can be rewritten as

$$\Delta n_{TPA} = \frac{1}{2}CL\delta I_o^2 \tag{4}$$

For pulsed excitation and a nonhomogeneous distribution of the intensity in the beam cross-section, I_o is a function of time and the transverse coordinate. In this case, eq 4 must be integrated over time and the laser beam radius to find the average excitation rate of the sample. After simple calculations, one can show that for a Gaussian beam the total excitation rate in the sample (ΔN_{TPA}) can be expressed as

$$\Delta N_{TPA} = \frac{\delta L C P_{av}^2}{2Af\hbar^2\omega^2\pi R^2\tau} \tag{5}$$

Here, P_{av} is the average power of the laser, R is the Gaussian diameter of the beam, τ is the pulse temporal full-width-at-half-maximum (fwhm), $\omega = 2\pi c/\lambda$ is the cyclic frequency of light (c is the speed of light and λ is the photon wavelength), and $\hbar$ is the reduced Planck constant. The coefficient A depends on the model used for the description of the laser pulse temporal shape. Also, A takes into account the Gaussian distribution of intensity in the laser beam cross-section. For a Gaussian pulse $A = 1.2\sqrt{2\pi} \approx 3$, and for a hyperbolic secant squared pulse $A \approx 3.41$. We assumed a Gaussian pulse shape in our calculations. The laser-pulse temporal fwhm was determined to be ~140 fs by a home-built single-shot autocorrelator. The average laser power inside the cell was determined by an external power meter and adjusted for the reflection losses by factoring in Fresnel reflection coefficients. The Gaussian radius of the beam was found to be ~0.13 cm by scanning a razor blade across the beam and monitoring the transmitted optical power vs the blade position. A two-photon excitation wavelength of 800 nm was used due to constraints on our laser system, which corresponds to $\delta = 343$ ($\pm 10\%$) GM. We note that larger excitation rates would be observed by exciting at shorter wavelengths (where δ is larger). Our TPIP demonstration is a proof of concept, and we have not attempted to optimize δ at our excitation wavelength.

Successful TPIP was observed after high pump-fluence exposure of bulk monomer solutions of the most effective co-initiator (triethylamine) and QDs (Table 1B). Experimental TPIP quantum yields are approximately a factor of 2 lower than those from the linear polymerization experiments. We believe that
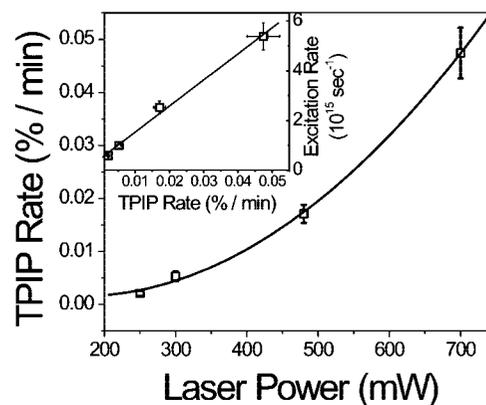
Figure 4. TPIP of MMA by QDs. Experimental TPIP rate as a function of laser power fitted to a second-order polynomial ($R^2 = 0.9991$, SD = 0.0011). TPIP rate follows a quadratic function of laser power. (Inset) TPIP rate vs calculated excitation rate (eq 5).

the TPIP quantum yield values are lower due to a more pronounced effect of inhibitors such as oxygen. Because lower conversion ranges are explored in TPIP experiments (typically ~1% conversion compared to ~10% in linear experiments), the induction period during which inhibitors are being destroyed represents a larger fraction of the total polymerization time. As a result, the experimental quantum yield values for TPIP are inherently lower than those of linear photopolymerization because a larger fraction of excitations are consumed by inhibitor removal. Lower Φ_o values observed within TPIP experiments at lower conversion ranges support this claim. Further, our experimental setup (in solution) allows inhibitor diffusion and therefore requires all inhibitors in the solution to be consumed. Conversely, in solid films (typical of TPIP applications) diffusion is arrested and inhibitor consumption is only necessary in the local area of excitation. Some inhibition of polymer formation due to oxygen and other inhibitors is unavoidable and is advantageous for applications where subdiffraction resolution is desired as inhibition spatially contains growing polymer.[5] Thus, TPIP applications would not likely be negatively affected by the degree of inhibitor sensitivity observed here.

Typically, the TPIP rate is predicted to scale with the square-root of the excitation rate ($\sqrt{\Delta N_{TPA}}$) and linearly with laser power.[7,25] Our observed TPIP rate scales linearly with the excitation rate, ΔN_{TPA}, and thus quadratically with laser power (Figure 4). This observation is explained by considering that the predicted square-root dependence is a product of intensity-dependent bimolecular chain termination rates. The higher-order dependence observed here indicates that changes in laser power (in the range explored here) do not significantly change the rate of bimolecular termination. The similar molecular weights of PMMA polymerized at different intensities of two-photon excitation are evidence supporting this claim, as it is expected that significant increases in excitation density will also decrease polymer molecular weight as was observed in linear polymerizations. Furthermore, the linear effect could be masked by the very gradual nonlinearity of the excitation rate in the intensity range explored. That is, a linear fit to the data in Figure 4 only deviates slightly from the quadratic fit shown. However, regardless of the subtleties of intensity-dependent rates of polymerization, TPIP using co-initiator-modified QDs was successfully demonstrated.
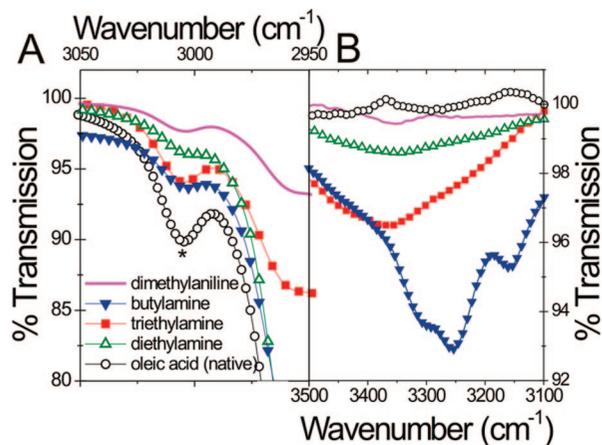
Figure 5. FTIR transmission spectra of ligand exchanged QD films. IR transmission spectrum of CdS QD films after treatment with various co-initiators all show (A) an absorbance decrease in the olefinic C–H stretching region denoted with a (*) indicative of partial oleic acid displacement. (B) The presence of new absorption bands above 3000 cm^{-1} shows a permanent binding of *n*-butylamine, whereas absorption due to diethylamine, triethylamine, and dimethylaniline (2,6-diisopropyldimethylaniline) are not observed.

QD Surface Derivatization. To gain further understanding of the underlying physical interactions (e.g., adsorption and displacement of native ligands) between co-initiators and QDs, we monitored the FTIR absorbance of co-initiator-treated QDs. We hypothesize that displacement of electronically passivating and sterically protective native oleic acid ligands is a prerequisite for efficient photoinitiation, and this hypothesis is supported by the inefficient polymerization observed in the absence of co-initiators. Detailed studies of the selected co-initiators and their ability to bind and displace native ligands on QD surfaces, however, are currently unavailable. Traditional ligand exchange, purification, and redispersal[27] could be carried out with select co-initiators (e.g., *n*-butylamine); however, others (e.g., triethylamine, diethylamine, and 2,6-diisopropyldimethylaniline) rendered the QDs insoluble during attempted ligand exchange due to the short length of the co-initiators or their (*sec-* or *tert-*) chemical structure. The inability to redisperse co-initiator treated QDs precludes solution-based studies (e.g., NMR) of QD/co-initiator binding interactions. Therefore, drop-cast QD films were investigated using FTIR absorbance spectroscopy after treatment with solutions of the chosen co-initiators or monomer and subsequent rinsing to remove unbound and weakly bound molecules (Figure 5).

A decrease in the intensity of the oleic acid olefinic C–H stretch (3010 cm^{-1}) is observed in all cases of amine co-initiator treatment indicating partial displacement and removal of oleic acid ligands. The carboxylate stretch of oleic acid is found at ~1550 cm^{-1}, shifted from its free position near ~1710 cm^{-1} due to the coordination with the CdS surface (see Supporting Information). Therefore, this stretch cannot be used to gauge native ligand removal due to the presence of other aliphatic C–H absorption bands occurring at these wavenumbers. It is known that *n*-butylamine[28] and other primary amines displace oleic acid and remain coordinated to semiconductor surfaces, and this is verified by the presence of N–H stretching features

above 3000 cm^{-1} after film treatment with n-butylamine. The presence of diethylamine is not detected (N–H stretch ~3250 cm^{-1}), and the small signal observed is due to adsorbed water or ethanol. IR absorption from tertiary amines (triethylamine and 2,6-diisopropyldimethylaniline) is not observed in the C–N stretching region (1210–1150 cm^{-1}, not shown). The weak absorption feature at 3400 cm^{-1} in the triethylamine-treated film is attributed to water or ethanol, as an N–H stretch is not possible. The 2,6-diisopropyldimethylaniline molecule presents strong absorption bands at unique wavenumbers relative to oleic acid due to the presence of the aromatic ring, but such absorbance bands are not observed. Therefore, we believe secondary and tertiary amines displace native oleic acid ligands but do not remain coordinated to the QD surface under these conditions of co-initiator treatment, rinsing with solvent and drying under an argon stream. The FTIR spectrum of the pyridine-containing molecule 4-dimethylaminopyridine is not shown because stable surface coordination and native ligand displacement have been previously verified for pyridines.[27] Exposure of QD films to MMA monomer (not shown for clarity) does not change the FTIR absorption spectrum of the QD films which further suggests there is little or no interaction between monomer, QD surface, or native ligands. We conclude that all of the co-initiators explored displace the native oleic acid ligands and therefore likely remain at least weakly bound to the QD surface in solution, whereas MMA monomer does not affect the oleic acid-capped QD surface.

QD Fluorescence Quenching. To better understand the QD exited-state interactions with co-initiators and monomer, we collected fluorescence-emission spectra of QDs in the presence of these molecules. We propose that QD band-edge emission competes directly with any photoinitiation event (e.g., radical formation) during polymerization reactions because all excitonic energy (~3.0 eV) is transferred to the emitted photon. Trap emission also likely competes directly with photoinitiation. First, it is unlikely that energy lost nonradiatively in the trapping process (0.5–1.25 eV, in this case) results in initiation. Second, the trap-mediated emission implies a decay of the trap state and, hence, the transfer of any remaining potential energy to the emitted photon via electron–hole recombination. Although emission quenching does not *imply* photoinitiation, emission quenching is a *consequence* of photoinitiation.[7] Therefore, fluorescence quenching is necessary for efficient photoinitiation.

Steady-state fluorescence spectra of QDs were recorded separately in the presence of the selected co-initiators and MMA monomer (Figure 6). The presence of MMA monomer shows no emission quenching, leaving the as-synthesized QD fluorescence spectrum unchanged. Although reduction[16] and oxidation[18] of MMA by photoexcited CdS has been reported, these processes are either inefficient or inactive, as they would otherwise result in fluorescence quenching. The inability of MMA monomer to quench QD emission is consistent with the inefficient photopolymerization in the absence of co-initiators. Contrary to the effects of MMA, all of the co-initiators examined strongly quench band-edge emission, presumably due to electron transfer from the amine to the CdS valence band hole.[29]

The effect of the amine co-initiators on the trap state emission, however, is highly dependent on their chemical structure. Tertiary amine co-initiators including triethylamine, 2,6-diisopropyldimethylaniline, diethylethylenediamine and 4-dimethylaminopyridine alter QD trap emission in differing ways

(27) Murray, C. B.; Norris, D. J.; Bawendi, M. G. *J. Am. Chem. Soc.* **1993**, *115*, 8706.

(28) Konstantatos, G.; Howard, I.; Fischer, A.; Hoogland, S.; Clifford, J.; Klem, E.; Levina, L.; Sargent, E. H. *Nature* **2006**, *442*, 180.
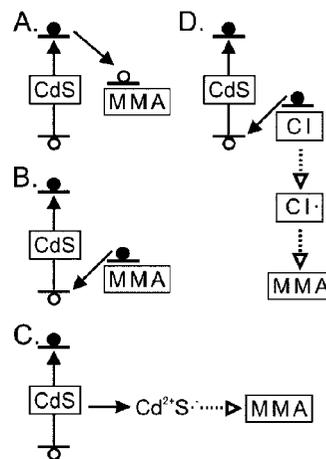
(29) Fox, M. A. *Acc. Chem. Res.* **1983**, *16*, 314.
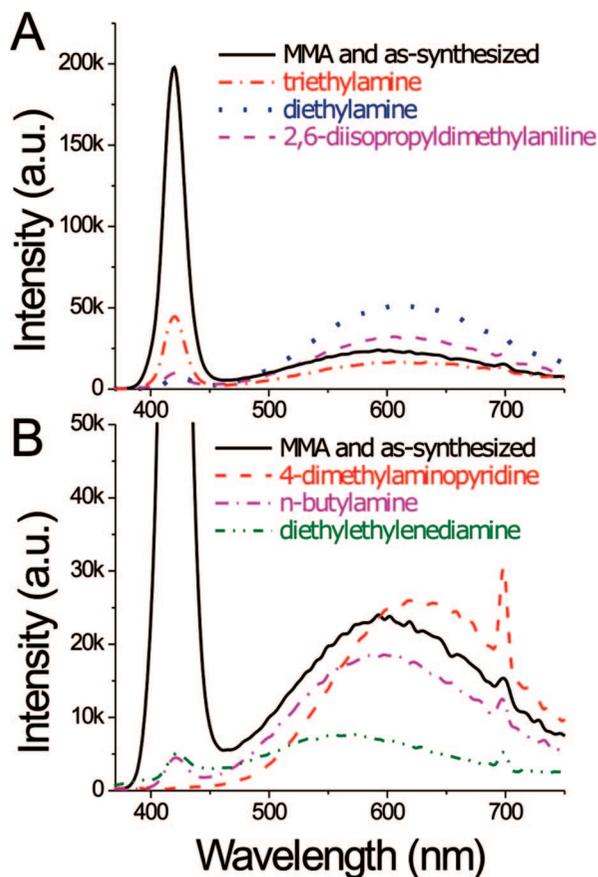
Figure 6. Fluorescence quenching by co-initiators. (A,B) CdS band edge emission is quenched by all co-initiators but not affected by MMA monomer. Several co-initiators increase trap emission whereas *tert*-alkyl-amines (triethylamine and diethylethylenediamine) quench trap emission. Coinitiators and monomer are present in equal concentration (225 mM).

Figure 7. Schematic of possible initiation mechanisms resulting from CdS QD photoexcitation. (A) Reduction of methymethacrylate (MMA) monomer, (B) oxidation of monomer, (C) surface radical generation and transfer to monomer, and (D) oxidation of co-initiator (CI) generating a radical that is transferred to monomer. Solid arrows indicate electron transfer, and dotted arrows indicate generation or transfer of radicals.

depending on the type of substituent. Triethylamine and diethylethylenediamine, which both possess *tert*-amines containing all alkyl substituents, quench trap emission. Conversely, 2,6-diisopropyldimethylaniline and 4-dimethylaminopyridine, which contain aromatic moieties, increase trap emission (see Supporting Information for integrated trap emission yields). Primary amines such as *n*-butylamine quench trap emission, whereas secondary amines greatly enhance trap emission. The trap emission spectra of QDs treated with the pyridine-containing molecules, such as 4-dimethylaminopyridine and 4-vinylpyridine (not shown), are shifted to slightly longer wavelengths.

The trap-state fluorescence is dependent on the co-initiator structure, which suggests that different co-initiator interactions with the photoexcited QDs are occurring. The observation that some amines, including triethylamine, quench trap state emission might suggest that these molecules interact more strongly with trapped carriers than the other co-initiators. Although the nature of this interaction is currently unknown, the differing interactions with the QD surface likely influence the ability of QD excitations to generate polymer-initiating free radicals and is discussed below.

Initiation Mechanisms. In consideration of possible photoinitiated polymerization mechanisms, it is useful to consider first the simplified case of photopolymerization in absence of co-initiators. The mechanism of QD-photoinitiation *without co-initiator modification* may occur through three possible processes following QD excitation (Figure 7): (A) via reduction of

monomer by a QD conduction band electron, (B) via oxidation of monomer by a QD valence band hole, or (C) via radical generation directly on the QD surface. Electron transfer (Process A)[7,16,17,20] and hole transfer (Process B)[16,18,19] from an excited photosensitizer have been previously reported to be responsible for photoinitiated polymerization of MMA.

Due to the apparent controversy regarding the initiation mechanism, we compare the redox potentials of the MMA monomer with the known energies of the CdS conduction and valence bands. Cyclic voltammetry performed on MMA monomer (Supporting Information) shows a reduction potential of approximately −2.1 V vs SCE. Based on the HOMO−LUMO gap of MMA (determined by optical absorption) of 4.1 eV, oxidation should occur at +2.0 V vs SCE. A wide range of valence band (or HOMO) levels have been reported for CdS (and CdS particles) ranging from +0.56[30] to +1.64 V[31] vs SCE. Because all reported valence band levels are significantly more negative than +2.0 V vs SCE, oxidation of MMA by the CdS valence band hole (Process B) is unlikely. Similarly, a large range of conduction band (or LUMO) levels have been reported ranging from −2.39[30] to −1.37 V vs SCE.[31] In the case of the more negative conduction band values, the reduction of MMA by the excited CdS QD conduction band electrons is thermodynamically favorable. Furthermore, the studies that reported the more negative CdS QD reduction potentials[30] (e.g., −2.39 V vs SCE) were conducted in organic solvent and utilized molecularly passivated QDs of similar size to those used in this work. Finally, photoinitiation occurring by radical production directly on the QD surface (Process C) cannot be ruled out. Such photoinduced radical formation has been observed on CdS through hole trapping and formation of S·⁻ radicals.[32–34] Although these processes (A and C) may be active, their ability to initiate polymerization is limited with unmodified QDs.

(30) Haram, S. K.; Quinn, B. M.; Bard, A. J. *J. Am. Chem. Soc.* **2001**, *123*, 8860.
(31) Xu, Y.; Schoonen, M. A. A. *Am. Mineral.* **2000**, *85*, 543.
(32) Kamat, P. V.; Ebbesen, T. W.; Dimitrijevic, N. M.; Nozik, A. J. *Chem. Phys. Lett.* **1989**, *157*, 384.
(33) Meissner, D.; Lauermann, I.; Memming, R.; Kastening, B. *J. Phys. Chem.* **1988**, *92*, 3484.
(34) Kamat, P. V. *Chem. Rev.* **1993**, *93*, 267.

Photosensitized polymerization *with amine co-initiator-modified* QDs can occur through one additional mechanism to those mentioned above (Figure 7): (D) via radical-generating oxidation of the co-initiator molecules. Because amines are used as co-initiators, reduction of the co-initiators is thermodynamically forbidden. Similarly, energy transfer from excited QDs to co-initiators is forbidden because the effective band gap of the QDs is less than the HOMO−LUMO gap of the co-initiators. Oxidation of the amine co-initiators readily occurs on the photoexcited QDs as evidenced by the efficient band-edge quenching observed. The oxidation of tertiary amines is reported to be responsible for radical formation and subsequent polymerization in other photosensitized polymerization systems.[35,36] It has been proposed that tertiary amines act through electron transfer to the excited sensitizer, followed by deprotonation of an amine α-carbon, radical formation, and transfer to monomer. We have conducted cyclic voltammetry and chronoamperometry studies on tertiary amines (e.g., triethylamine) in the presence of O_2-free monomer and did indeed observe irreversible oxidation of triethylamine (at +0.18 V vs SCE). However, no polymer was formed even after many ($\sim 10^{18}$) oxidation events, indicating that oxidation of the amine (on a platinum electrode) does not produce radicals capable of polymerizing MMA. Although this observation provides evidence against Process D, this mechanism cannot be ruled out because chemical transformations induced by photochemical oxidation on a semiconductor may be different than those induced electrochemically on metal electrodes. That is, photochemical oxidation of tertiary amines by CdS may yield polymer-initiating radicals whereas electrochemical oxidation of tertiary amines on a metal electrode does not.

However, the observed enhancement in polymerization efficiency due to the presence of amine co-initiators may also be due to the promotion of an already-active process (i.e., Processes A or C). Coinitiator-induced promotion of Process A (MMA reduction) can occur through increased accessibility of MMA to the surface (due to native ligand removal) and/or increased rates of MMA reduction due to the sacrificial oxidation of the amines. Promotion of Process C (radical formation directly on the QD surface) could occur through some combination of increased accessibility of monomer to CdS surface radicals, promotion of the generation of surface radicals, and mediation (by co-initiator) of surface radicals from CdS surface to monomer. Thus, the radical-forming de-excitation pathways active without co-initiator modification may be promoted by amine co-initiators.

We propose that generation of surface radicals via trapped carriers (Process C) is most likely the dominant initiation process for the following reasons. First, triethylamine was both a quencher of trap state fluorescence as well as the most effective co-initiator, which suggests that interaction with trap states is important for efficient initiation. Second, if Process A (direct MMA reduction) was the primary initiation mechanism, at least partial fluorescence quenching would be expected to coincide with polymer initiation. Because no band edge or trap state QD fluorescence quenching was observed upon MMA exposure, but polymerization was observed, we believe that band edge and emissive trap states are not *directly* involved in the photoinitiation. Therefore, nonemissive trap states are probably responsible for photoinitiation (Process C). A further mechanistic understanding of co-initiator-promoted QD-photosensitized polymerization is currently under investigation in our laboratory.

4. Conclusions

QD-sensitized one- and two-photon induced polymerization of MMA was demonstrated by employing surface-modifying co-initiators that were found to increase the efficiency of initiation and overall polymerization rates. This investigation of the photoinduced reactions and surface chemistry of semiconductor QDs yields information important for other photosensitization schemes including photodynamic therapy,[37,38] photoelectrochemical cells,[39] and photocatalysis.[29] For example, photodynamic therapy requires efficient generation of toxic radicals whereas photocatalysis and photoelectrochemical cells require efficient charge separation. All of these processes involve charge or energy transfer across the semiconductor surface and are highly dependent on the nature of that surface. Surface modification is therefore useful in influencing and understanding the outcome (e.g., radical formation, charge transfer, or photon emission) of excitations in nanostructured semiconductors.

The quantum efficiency for polymer initiation obtained in this study ($\Phi_o = 0.05$) is comparable to values reported for designer organic photosensitizers ($\Phi_o = 0.03$).[9] The quantum efficiencies for initiation demonstrated in both of these cases are still relatively small and leave considerable room for improvement. Notably, the TPA cross-sections of CdS QDs ($\delta = 3.5 \times 10^4$ GM) are significantly larger than large-δ organic photosensitizers ($\delta = 1250$ GM).[9] We do note, however, that the mass-normalized TPA cross sections of the QD photosensitizers (0.45 GM mol/g) are still lower than those of champion organic photosensitizers (1.9 GM mol/g). Although reports of molecular TPA cross-sections greater than 7×10^3 GM have been reported,[40–42] there are no reports of the use of those absorbers in TPIP, to the best of our knowledge. Further, the synthesis and purification of the QD photosensitizers is simple and requires only several hours. The solubility of QD sensitizers can also be tailored to various solvents based on simple solution-based ligand exchange, and loadings of higher than 10 wt % can be routinely obtained. Because the overall efficiency of a TPIP system depends on the product of δ and Φ_o, the demonstrated QD/co-initiator system is competitive with champion organic two-photon sensitizers and is worthy of further investigation. We are currently working to further understand the photosensitized initiation mechanisms as well as extend the chemistry shown here to semisolid films of multifunctional monomers, QDs, and co-initiators.

(35) Bi, Y. B.; Neckers, D. C. *Macromolecules* **1994**, *27*, 3683.
(36) Sandner, M. R.; Osborn, C. L.; Trecker, D. J. *J. Polym. Sci., Part A: Polym. Chem.* **1972**, *10*, 3173.
(37) Ipe, B. I.; Lehnig, M.; Niemeyer, C. M. *Small* **2005**, *1*, 706.
(38) Bakalova, R.; Ohba, H.; Zhelev, Z.; Ishikawa, M.; Baba, Y. *Nat. Biotechnol.* **2004**, *22*, 1360.
(39) Robel, I.; Subramanian, V.; Kuno, M.; Kamat, P. V. *J. Am. Chem. Soc.* **2006**, *128*, 2385.
(40) Kim, D. Y.; Ahn, T. K.; Kwon, J. H.; Kim, D.; Ikeue, T.; Aratani, N.; Osuka, A.; Shigeiwa, M.; Maeda, S. *J. Phys. Chem. A* **2005**, *109*, 2996.
(41) Ogawa, K.; Ohashi, A.; Kobuke, Y.; Kamada, K.; Ohta, K. *J. Phys. Chem. B* **2005**, *109*, 22003.
(42) Ahn, T. K.; Kim, K. S.; Kim, D. Y.; Noh, S. B.; Aratani, N.; Ikeda, C.; Osuka, A.; Kim, D. *J. Am. Chem. Soc.* **2006**, *128*, 1700.

Supporting Information Available: Additional fluorescence data, IR characterization, TPA cross-section measurements, electrochemical data, and complete ref 7. This material is available free of charge via the Internet at http://pubs.acs.org.

JA711295K